RadioGraphics

Multidetector CT Arthrography of the Wrist Joint: How to Do It[1]

Thomas Moser, MD • Jean-Claude Dosch, MD • Akli Moussaoui, MD Xavier Buy, MD • Afshin Gangi, MD, PhD • Jean-Louis Dietemann, MD

CME FEATURE

See accompanying test at http://www.rsna.org/education/rg_cme.html

LEARNING OBJECTIVES FOR TEST 2

After reading this article and taking the test, the reader will be able to:

- Identify the main ligaments of the wrist and the principal abnormalities of the bone, cartilage, and ligaments at multidetector CT arthrography.
- Describe the pathophysiologic mechanisms of wrist ligament tears and instability.
- Discuss articular injection technique and the imaging parameters for multidetector CT arthrography.

TEACHING POINTS

See last page

With its exquisite spatial resolution, multidetector computed tomographic (CT) arthrography of the wrist is a valuable tool for the diagnosis and evaluation of a wide spectrum of articular disorders. Traumatic tears of the interosseous ligaments can be classified as complete or incomplete and as partial- or full-thickness tears at multidetector CT arthrography and can also be differentiated from asymptomatic degenerative lesions. In addition, tears of the triangular fibrocartilage complex can be differentiated according to their location. A tailored contrast material injection technique and multiplanar reformation are recommended for optimal assessment of these structures. Multidetector CT arthrography is also remarkably effective in demonstrating cartilage and bone abnormalities, many of which cannot be depicted with other imaging techniques. The chief limitation of multidetector CT arthrography lies in the evaluation of soft-tissue abnormalities, which may benefit from the addition of other imaging techniques such as ultrasonography or magnetic resonance imaging. A basic knowledge of the relevant anatomy, pathophysiologic features, and imaging technique is mandatory for obtaining high-yield diagnostic information concerning the wrist joint.

Abbreviations: DRUJ = distal radioulnar joint, TFCC = triangular fibrocartilage complex

RadioGraphics 2008; 28:787–800 • **Published online** 10.1148/rg.283075087 • **Content Codes:** CT MK

[1]From the Department of Radiology, Strasbourg University Hospital, 1 Place de l'Hôpital, 67000 Strasbourg, France. Recipient of a Certificate of Merit award for an education exhibit at the 2006 RSNA Annual Meeting. Received April 30, 2007; revision requested June 28 and received September 6; accepted September 24. All authors have no financial relationships to disclose. **Address correspondence to** T.M. (e-mail: *thomas.moser@chru-strasbourg.fr*).

Introduction

Multidetector computed tomographic (CT) arthrography of the wrist joint is a recently developed technique that has not received much attention in the literature (1,2). It largely derives from conventional arthrography but benefits from the advances of new-generation multidetector CT. Submillimeter isotropic imaging is particularly useful in demonstrating tiny normal structures of the wrist and the disorders that affect them. Thus, multidetector CT arthrography represents a viable alternative to magnetic resonance (MR) imaging and MR arthrography, the principal imaging modalities performed for such indications (3,4).

In this article, we review the normal anatomy of the wrist joint and the pathophysiologic bases of wrist ligament tears. In addition, we describe injection and imaging technique. We also discuss and illustrate the normal multidetector CT arthrographic findings in the wrist, as well as the imaging features of various ligament tears and of abnormalities of the cartilage, bone, and soft tissue.

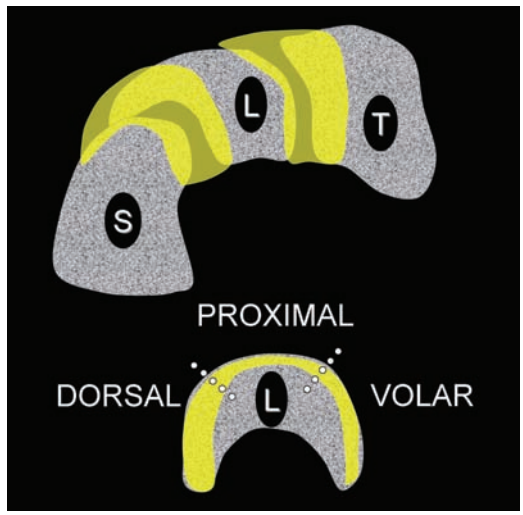

Figure 1. Drawings illustrate how the scapholunate and lunotriquetral ligaments (yellow) are essential in linking the bones of the proximal carpal row (*L* = lunate bone, *S* = scaphoid bone, *T* = triquetral bone) (top), and how each horseshoe-shaped ligament consists of three functionally distinct portions: volar, proximal, and dorsal (sagittal view, bottom). The membranous proximal portion has very limited biomechanical value.

Normal Anatomy of the Wrist Joint

Teaching Point

The wrist joint is considered to be the most complex articulation in the human body. However, its anatomy can be simplified into three major compartments: the distal radioulnar joint (DRUJ), the radiocarpal joint, and the midcarpal joint. The radiocarpal joint involves the distal radius and the proximal carpal row; the midcarpal joint involves the proximal and distal carpal rows. Their combined motion is synergistic and comparable to that of a spheroidal joint, allowing flexion (volar flexion), extension (dorsal flexion), and radial and ulnar deviations of the wrist. Along with its proximal counterpart, the DRUJ is responsible for pronation and supination of the forearm. With the exception of the first carpometacarpal joint, other joint spaces have less functional importance, since the common carpometacarpal joint solidly attaches the distal carpal row to the second through the fifth metacarpal bases (5).

Nevertheless, this simplified conception of the wrist anatomy underlines the importance of the proximal carpal row for wrist mobility. Because of its location between the distal radius and the distal carpal row, it acts as an intercalated segment (5). The adjacent bones of the proximal carpal row are linked by the interosseous scapholunate and lunotriquetral ligaments. These ligaments are horseshoe shaped with three functionally distinct portions: volar, proximal, and dorsal (Fig 1). By merging anteriorly and posteriorly with the articular capsule, the ligaments seal off the radiocarpal and midcarpal compartments (6).

The triangular fibrocartilage complex (TFCC) is another key anatomic structure. The TFCC is located on the ulnar side of the wrist and includes the extensor carpi ulnaris tendon sheath, the dorsal radioulnar ligament, the triangular fibrocartilage proper, the volar radioulnar ligament, the ulnocarpal ligaments (ulnolunate and ulnotriquetral), the ulnar collateral ligament, and the meniscus homologue. These structures are devoted to the stabilization of the DRUJ and the ulnar aspect of the wrist, as well as the transmission of the load through the ulnar side of the wrist (7). The triangular fibrocartilage seals off the DRUJ from the radiocarpal joint. The thickness of its central portion, interposed between the ulnar head and the medial aspect of the lunate bone, is only a few millimeters and is inversely proportional to the ulnar variance (8).

The wrist joint is limited by a fibrous capsule reinforced by strong fascicles known as capsular ligaments. These structures are important secondary stabilizers of the wrist joint. On the volar side of the wrist, it is usually possible to differentiate

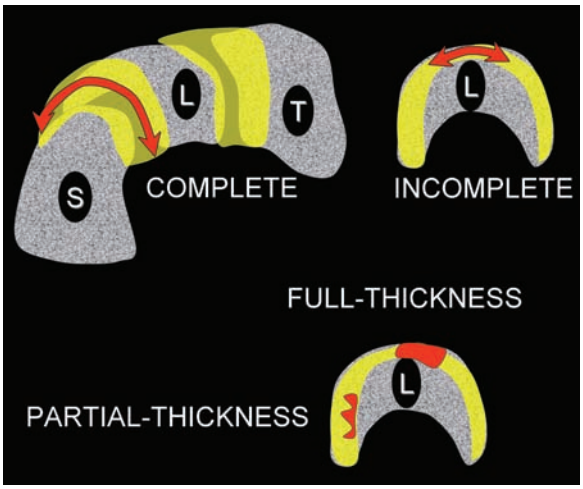

Figure 2. Drawings illustrate the classification of interosseous ligament tears (red). These tears are classified as complete when all three portions of a ligament (yellow) are disrupted (upper left) and as incomplete when only one or two portions are disrupted (upper right). Ligament tears are further classified as full-thickness or partial-thickness tears (bottom). *L* = lunate bone, *S* = scaphoid bone, *T* = triquetral bone.

between the "proximal V," which consists of the long radiolunate and ulnolunate ligaments, and the "distal V," which consists of the radioscaphocapitate, ulnotriquetral, and triquetrocapitate ligaments (9). A "lateral V" formed by the radiocarpal and intercarpal ligaments is seen on the dorsal side of the wrist (10). Alternative nomenclature for these ligaments as well as descriptions of numerous additional fascicles can be found in the literature, but the aforementioned ligaments are the most important with which to be familiar.

Pathophysiologic Bases of Wrist Ligament Tears

Because of its intercalated situation and wide range of motion, the proximal carpal row is largely exposed to acute or repetitive trauma. The most common mechanism of acute trauma is a fall on an outstretched hand, causing hyperextension and intercarpal supination. The resulting pattern of lesions is known as perilunate instability, which can be classic (starting from the scapholunate joint) or reverse (beginning in the lunotriquetral joint), depending on whether the impact is thenar (abducted arm) or hypothenar (adducted arm). Associated tears of the scapholunate ligament, lunotriquetral ligament, and capsular ligaments may be seen (11).

Teaching Point

Precise delineation of the extent of a tear is feasible with modern imaging techniques, and most authors now differentiate between complete (all three portions disrupted) and incomplete (one or two portions disrupted, also referred to as "partial" by some authors) interosseous ligament tears (1,12,13). This distinction is clinically relevant, since most patients who present with incomplete tears have no wrist instability and can be treated conservatively (14,15). Experimental studies have demonstrated that disruption of both interosseous and capsular ligaments is needed to cause wrist instability (16,17). However, not all incomplete tears are equally negligible. The dorsal portion of the scapholunate ligament and the volar portion of the lunotriquetral ligament are essential for wrist stability, whereas the membranous proximal portions have virtually no mechanical importance (6,18). Further classification of ligament tears helps differentiate full-thickness (usually communicating) tears from partial-thickness (noncommunicating) tears (Fig 2). The pathologic significance of partial-thickness tears for interosseous ligaments is discussed in the literature, but the significance of such tears is widely considered to be greater for the TFCC (19,20).

Ligament disruptions are not always traumatic, and the prevalence of degenerative tears increases with age. Degenerative tears principally involving the proximal portions of the scapholunate and lunotriquetral ligaments and the central portion of the triangular fibrocartilage reflect the normal senescence of fibrocartilages. These tears are present in nearly one-half of the population over 50 years of age (21,22), are usually asymptomatic, and should be differentiated from traumatic tears. On the other hand, tears involving the dorsal portion of the scapholunate ligament or the ulnar insertion of the TFCC regularly cause symptoms (20,23).

Injection Technique: Choice of Puncture Site and Contrast Medium

At conventional arthrography of the wrist, ligament tears classically manifest as abnormal communication between adjacent compartments. Various imaging strategies have been proposed. Radiocarpal enhancement alone was considered insufficient due to the risk of false-negative results. However, true unidirectional communications are actually uncommon and are most frequently related to technical factors (24). Enhancement of the midcarpal compartment or DRUJ reportedly has a higher sensitivity for demonstrating interosseous ligament tears and TFCC tears, respectively (25,26). Therefore, triple-compartment arthrography was considered the most sensitive technique for demonstrating

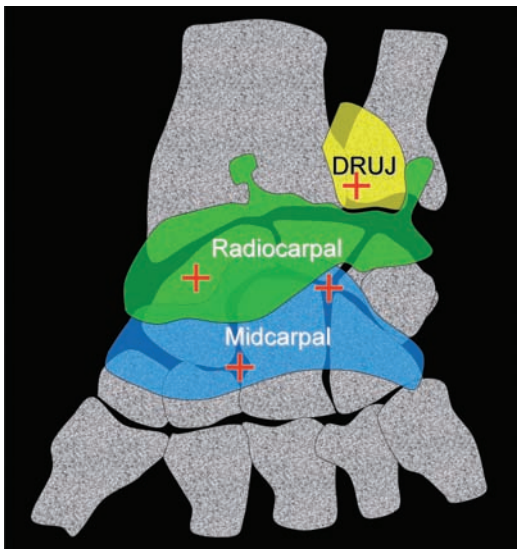

Figure 3. Drawing illustrates puncture sites (+) on the dorsal aspect of the wrist joint. The midcarpal compartment is punctured first, either between the scaphoid, trapezoid, and capitate bones or between the lunate, triquetral, capitate, and hamate bones. The DRUJ is punctured on the distal and radial aspect of the ulnar head whenever a TFCC tear is suspected. The radiocarpal compartment is punctured on the waist of the radius if it has not already enhanced through a tear.

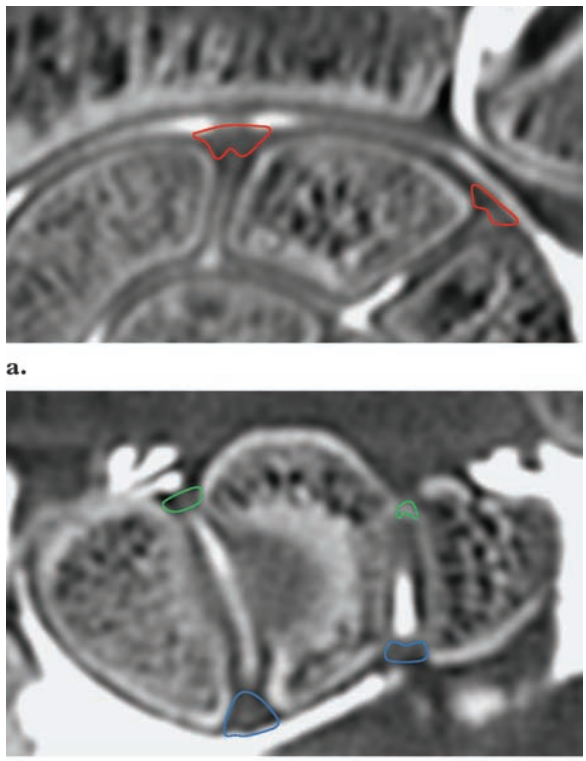

Figure 4. **(a)** Coronal multidetector CT arthrogram clearly shows the proximal portions of the interosseous scapholunate and lunotriquetral ligaments (outlined in red), with their cartilaginous insertion and meniscoid shape. **(b)** Transverse multidetector CT arthrogram shows the dorsal (outlined in blue) and volar (outlined in green) portions of the ligaments, with their bone insertion and flat shape.

abnormal communications, although lacking specificity for discriminating between traumatic and degenerative tears (27,28).

Teaching Point

Multidetector CT arthrography currently allows the direct visualization of ligament tears. Even partial-thickness tears can be recognized when both adjacent compartments are enhanced. The classic abnormal communication has actually lost its semeiologic importance, since ligament tears are directly visualized. Our examination protocol typically includes initial enhancement of the midcarpal compartment and, if a TFCC tear is suspected, enhancement of the DRUJ. The radiocarpal compartment is punctured only if spontaneous enhancement through a tear does not occur (1,28).

The dorsal aspect of the wrist is prepared sterilely and positioned horizontally under vertical fluoroscopic guidance. Local anesthetic is not used. Puncture is made with a 24-gauge needle and is greatly facilitated by targeting articular recesses rather than joint spaces (Fig 3). On average, a total of 5 mL of iodinated contrast medium is injected. The concentration should be lower than 300 mg of iodine per milliliter to avoid beam-hardening artifacts with multidetector CT. The patient is immediately directed to the multidetector CT suite to avoid excessive dilution of contrast medium.

Imaging Technique: Optimization of Multidetector CT Acquisition and Reconstruction Parameters

The patient is scanned in the "superman" position so that the wrist is in the middle of the gantry. The upper arm should be fully extended to counteract radial or ulnar deviation of the wrist. Excessive dorsal flexion of the wrist should also be avoided.

Technical parameters are set to achieve the highest spatial resolution. The thinnest possible beam collimation (0.5 mm) is used in conjunction with a shallow pitch. In our experience with matrix array multidetector CT, adequate image quality is achieved with use of all detector rows (ie, 64 × 0.5-mm collimation), thereby reducing scanning time and limiting motion artifacts. Reconstruction makes use of a high-frequency

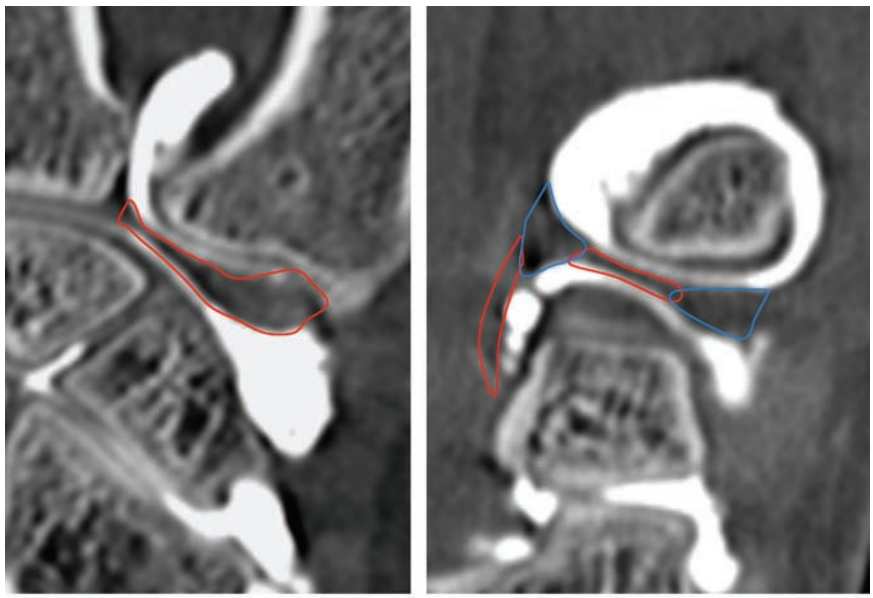

a. b.

Figure 5. **(a)** Coronal multidetector CT arthrogram clearly depicts the triangular fibrocartilage proper (outlined in red). **(b)** Sagittal multidetector CT arthrogram also shows the triangular fibrocartilage proper (horizontal area outlined in red), along with the dorsal and volar distal radioulnar (outlined in blue) and ulnocarpal (vertical area outlined in red) ligaments.

kernel and a substantial section overlap (eg, 0.2-mm increments in our protocol). A small field of view (~100 mm) is selected to achieve a voxel size of approximately 0.2 mm. Exposure parameters are 100 kV and 100 mAs.

Isotropic acquisition allows optimal reformation in virtually any plane. Corrected transverse, sagittal, and coronal reformatted images are routinely obtained along the axis of the capitate bone. Coronal images provide a practical overview of the wrist joint, whereas transverse images are essential for appreciating the functionally important dorsal and volar portions of the interosseous ligaments, and sagittal images provide a good analysis of the TFCC.

Normal Imaging Findings

Interosseous Scapholunate and Lunotriquetral Ligaments

The scapholunate and lunotriquetral ligaments seal their respective joint spaces, thereby sealing off the radiocarpal and midcarpal compartments. The three portions of these ligaments are demonstrated consistently and reliably with multidetector CT arthrography. The proximal portions are well seen on coronal images (Fig 4a), whereas the dorsal and volar portions can be analyzed on transverse images (Fig 4b). The normal appearance of these ligaments has been well studied with MR imaging and can easily be transposed to multidetector CT arthrography (29–31). Variations in shape (flat or meniscoid) and mode of insertion (on bone, cartilage, or both) depend on the portion of the ligament under consideration: The proximal portions are usually meniscoid and insert on cartilage, whereas the dorsal and volar portions are more often flat and insert on bone. These features are easily recognized at multidetector CT arthrography. On the other hand, variations in signal intensity at MR imaging are not relevant at multidetector CT arthrography, especially when they are interstitial. However, particular attention should be paid to the margins of the ligaments, since subtle abnormalities can reveal partial-thickness tears or cicatricial ligament.

Triangular Fibrocartilage Complex

The TFCC is adequately analyzed with multidetector CT arthrography. The fibrocartilage proper is clearly seen on a coronal image from its cartilaginous insertion on the radial sigmoid notch to its ulnar attachment (Fig 5a). This ulnar attachment consists of two different fascicles that insert on the base and tip of the styloid process, respectively, and are separated by loose fibrovascular tissue that can mimic a tear at MR imaging (32). These fascicles cannot be differentiated with multidetector CT arthrography. The anterior and posterior distal radioulnar ligaments, as well as the ulnocarpal ligaments, are well seen on sagittal images (Fig 5b).

Capsular Ligaments

The capsular ligaments are also visualized at multidetector CT arthrography, although they

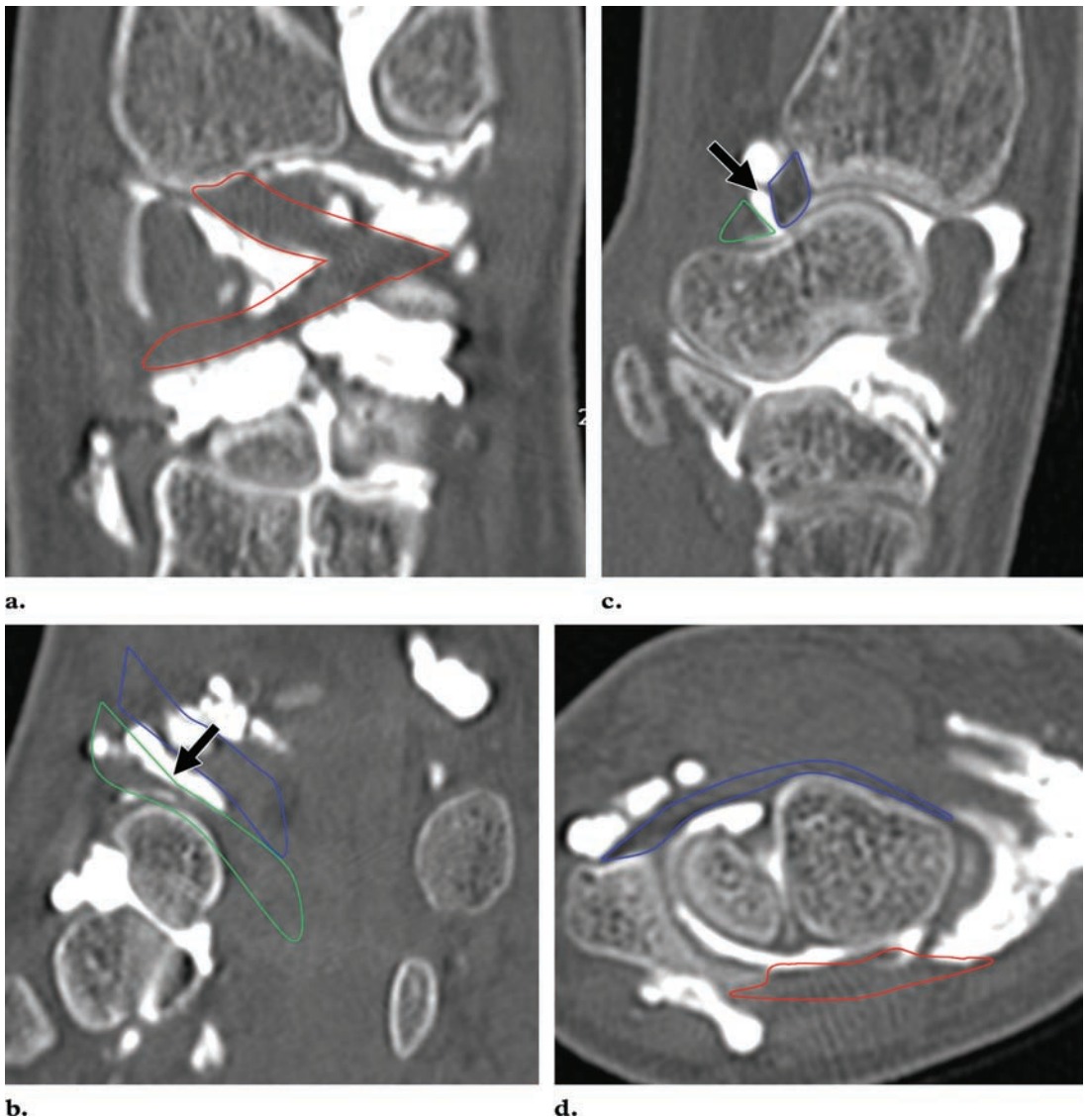

Figure 6. **(a)** Coronal multidetector CT arthrogram shows the dorsal radiocarpal and intracarpal ligaments (outlined in red). **(b, c)** Coronal **(b)** and sagittal **(c)** multidetector CT arthrograms show the palmar long radiolunate (outlined in blue) and radioscaphocapitate (outlined in green) ligaments. A recess known as the Poirier space (arrow) separates these two ligaments and represents an area of capsular weakness. **(d)** Transverse multidetector CT arthrogram shows the dorsal radiocarpal (outlined in red) and palmar long radiolunate (outlined in blue) ligaments.

are less conspicuous than at MR imaging or MR arthrography. Coronal and transverse images are useful, since many of these ligaments are seen almost entirely on a single image (Fig 6). Sagittal imaging helps evaluate these ligaments more precisely in cross section. The long radiolunate and radioscaphocapitate ligaments are invariably seen on sagittal images, separated by the capsular recess of Poirier. It is particularly important to evaluate this region of capsular weakness because its disruption from impaction by the capitate head occurs with hyperextension trauma.

Bone Variants

A small number of normal bone variants are regularly seen at multidetector CT arthrography of the wrist joint and should not be mistaken for pathologic conditions. Cystlike defects are focal areas of hypoattenuation in bone that often communicate with the joint through a limited cortical aperture. These defects represent either vascular channels or intraosseous ganglion cysts. Bone islands have typical features that are not specific to carpal bones (33).

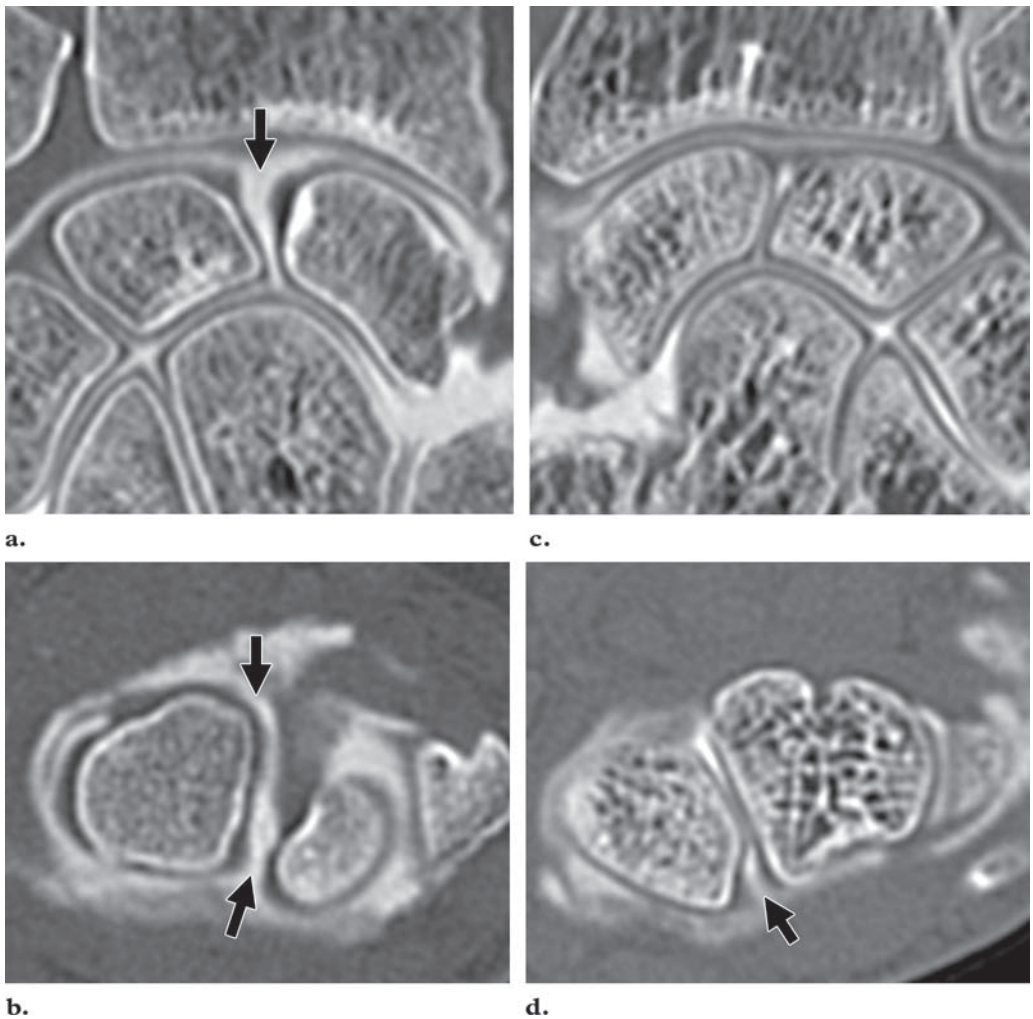

Figure 7. Complete versus incomplete tear of the scapholunate ligament. **(a, b)** Complete tear. **(a)** Coronal multidetector CT arthrogram shows disruption of the proximal portion of the scapholunate ligament (arrow). **(b)** Transverse multidetector CT arthrogram shows disruption of the volar and dorsal portions of the ligament (arrows). **(c, d)** Incomplete tear in a different patient. **(c)** On a coronal multidetector CT arthrogram, the proximal portion of the ligament is intact. **(d)** Transverse multidetector CT arthrogram shows a tear involving the dorsal portion of the ligament (arrow), with the volar portion intact.

A carpal coalition is another classic variant, most commonly involving the lunotriquetral space. Such a coalition can be complete but can also be partial and mimic osteoarthritis. A useful clue to the diagnosis is the invariable partial development of the joint space on its distal aspect (from a simple bone notch to true cartilaginous facets) (34).

Ligament Tears

Interosseous Scapholunate and Lunotriquetral Ligament Tears

In our experience, suspicion for scapholunate or lunotriquetral ligament tears represents the most common indication for multidetector CT arthrography. As mentioned earlier, scapholunate and lunotriquetral ligament tears are classified as either complete or incomplete depending on whether all three portions are disrupted. This distinction is easily made with multiplanar reformation (Fig 7).

Teaching Point

A tear varies in appearance depending on its extent. Full-thickness tears are usually communicating (unless the defect is plugged by a scar) and manifest as an interruption of the ligament underlined by iodinated contrast material. The stump of the ligament can be seen floating freely in cases of recent tear but then progressively disappears over time. Assessment of the stump can be useful for guiding reconstructive surgery. Partial-thickness tears are noncommunicating and therefore require enhancement of both adjacent compartments for adequate depiction. They manifest as abnormal thinning, superficial fraying, or irregularities on one side of the ligament (Fig 8a, 8b). Ganglion cyst formation from a partial-thickness tear is also frequently observed in the dorsal portion of the scapholunate ligament. These cysts can be very small and unenhanced, being identified only on the basis of focal bulging of the dorsal scapholunate ligament in its lower aspect (Fig 8c, 8d).

a.

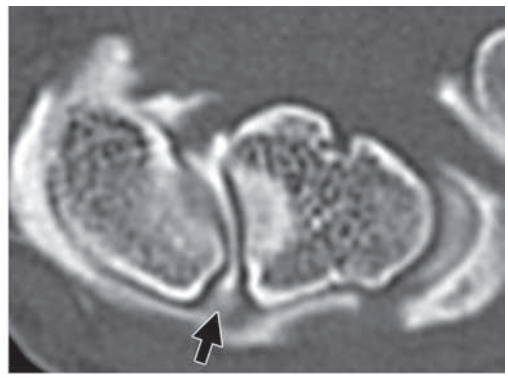

b.

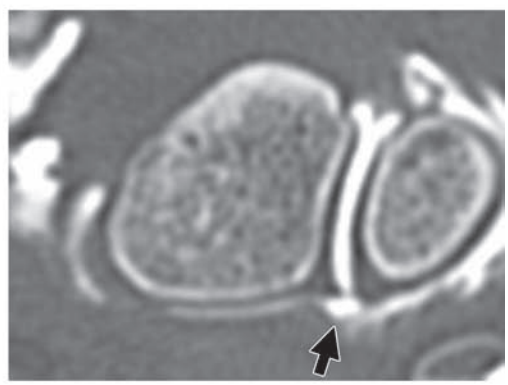

c.

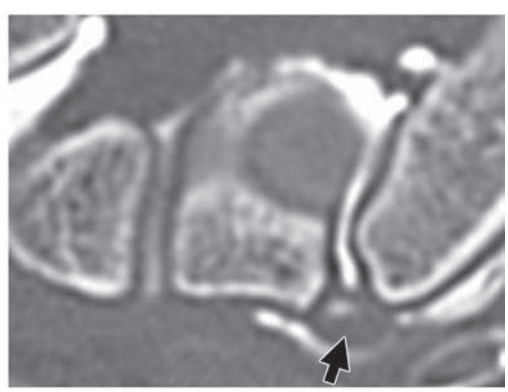

d.

Figure 8. Partial-thickness tears of the scapholunate ligament. **(a)** Coronal multidetector CT arthrogram shows a degenerative partial-thickness tear manifesting as marked thinning of the proximal portion of the scapholunate ligament (arrow). **(b)** Transverse multidetector CT arthrogram obtained in a different patient shows a partial-thickness tear manifesting as irregularities of the dorsal portion of the ligament (arrow). **(c, d)** Transverse multidetector CT arthrograms obtained in a third patient show a partial-thickness tear of the dorsal portion of the ligament with cyst formation (arrow).

Moreover, indirect signs of instability can be present and generally represent complete interosseous and associated capsular ligament tears. These signs include scapholunate diastasis, abnormal scapholunate angle, instability patterns of the dorsal or volar intercalated segment, and rotatory subluxation of the scaphoid bone (35,36).

TFCC Tears

TFCC tears are routinely classified according to the system developed by Palmer (37). Class I lesions are presumed to be traumatic, with type IA characterized by a slitlike central perforation (Fig 9a, 9b); type IB, by an ulnar avulsion (equivalent to a fracture of the base of the ulnar styloid process) (Fig 9c); type IC, by a distal avulsion of the ulnocarpal ligaments; and type ID, by a radial avulsion with possible sigmoid notch fracture. Class II lesions are considered degenerative and result from chronic ulnocarpal impaction. A chronologic progression of lesions has been described, with type IIA corresponding to central wear of the triangular fibrocartilage (Fig 10a); type IIB, to additional ulnar or lunate chondro-

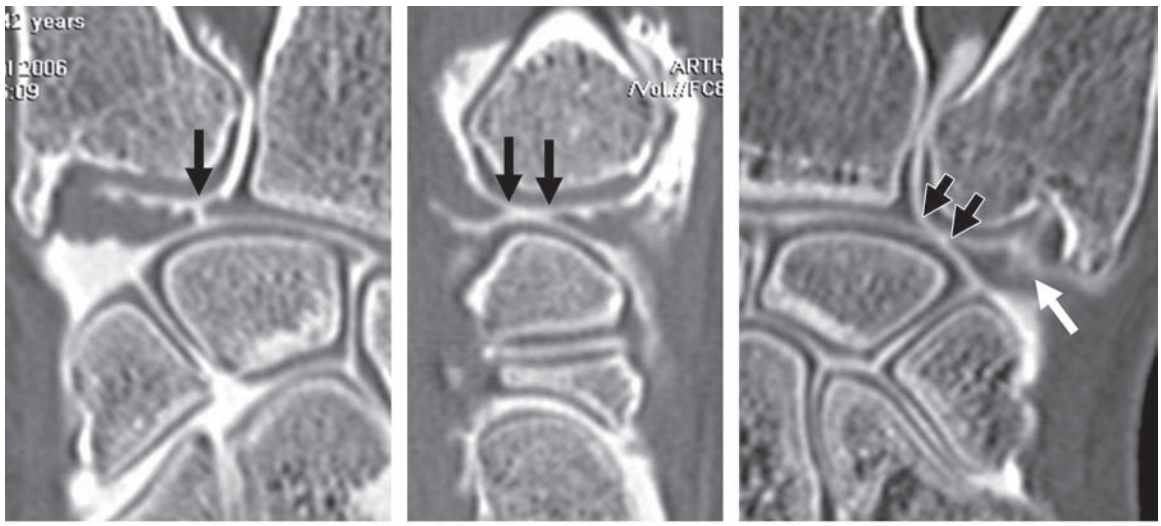

a. b. c.

Figure 9. Traumatic tears of the TFCC. **(a, b)** Coronal **(a)** and sagittal **(b)** multidetector CT arthrograms show a central slitlike tear (Palmer class IA) of the TFCC (arrows). **(c)** Coronal multidetector CT arthrogram obtained in a different patient shows an ulnar tear (class IB) (white arrow) with an associated degenerative central tear (class IIC) (black arrows).

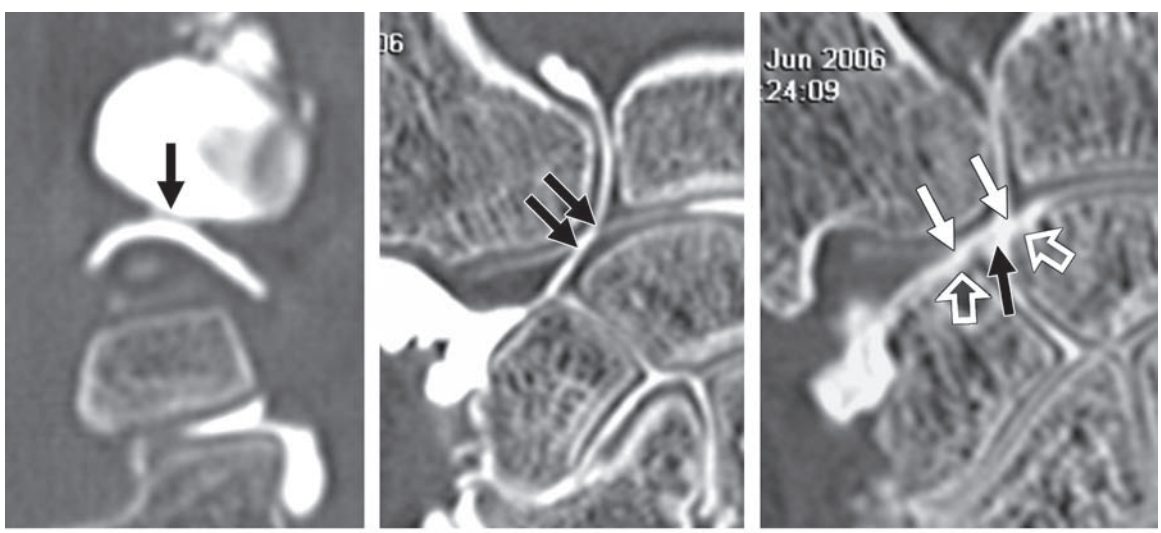

a. b. c.

Figure 10. Degenerative tears of the TFCC. **(a)** Sagittal multidetector CT arthrogram shows central wear (Palmer class IIA) of the triangular fibrocartilage (arrow). **(b)** Coronal multidetector CT arthrogram obtained in a different patient shows a central tear (class IIC) of the triangular fibrocartilage (arrows). **(c)** Coronal multidetector CT arthrogram obtained in a third patient also shows a central tear of the triangular fibrocartilage (solid white arrows), along with lunate and triquetral chondromalacia (open white arrows) and a lunotriquetral ligament tear (class IID) (black arrow).

malacia; type IIC, to an additional central tear of the triangular fibrocartilage (Figs 9c, 10b); type IID, to an additional lunotriquetral ligament tear (Fig 10c); and type IIE, to additional ulnocarpal osteoarthritis.

The principal advantage of this classification scheme lies in its description of the most common lesions. However, the distinction between traumatic and degenerative tears is not always straightforward, particularly in tears involving the radial aspect of the triangular fibrocartilage (20). Chondromalacia is not always associated with central perforation of the triangular fibrocartilage. In addition, DRUJ instability associated with disruption of the distal radioulnar ligaments is not included in this classification scheme. For these reasons, we routinely describe tears of the TFCC in terms of the elements involved and the extent of the tear without addressing their traumatic or degenerative nature.

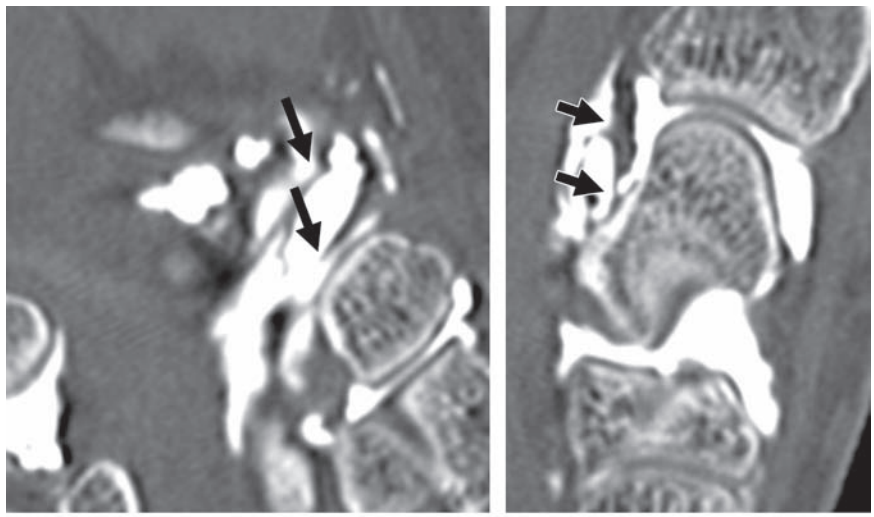

Figure 11. Capsular ligament tears. Coronal **(a)** and sagittal **(b)** multidetector CT arthrograms show disruption of the radioscaphocapitate and long radiolunate ligaments (arrows).

Capsular Ligament Tears

Capsular ligament tears are not consistently seen at imaging, particularly when the examination is delayed following trauma. Disruption of the long radiolunate and radioscaphocapitate ligaments is the most frequent manifestation (Fig 11). Avulsion fracture of the posterior triquetral tuberosity is equivalent to a dorsal capsular ligament tear.

Cartilage Abnormalities

Teaching Point

Cartilage abnormalities are exquisitely depicted with multidetector CT arthrography. Acute traumatic lesions are usually associated with articular fractures (Fig 12). Persistent incongruity is a major source of articular derangement, and the maximum tolerable step-off is less than 2 mm (Fig 13). Early cartilage degeneration also occurs as a result of loss of radial inclination and volar tilt or radial shortening with relative lengthening of the ulna (38). Degenerative lesions are the result of excessive strain over articular surfaces caused by posttraumatic instability or malalignment. Various patterns can be recognized, including radioscaphoid osteoarthritis, ulnocarpal impaction syndrome, and hamatolunate impingement.

Radioscaphoid Osteoarthritis

Degenerative changes in the radiocarpal joint commonly affect the radioscaphoid compartment, beginning around the radial styloid process and progressively extending to the scaphoid fossa. Two principal patterns are recognized: scapholunate advanced collapse and scaphoid nonunion advanced collapse. Scapholunate advanced collapse is a consequence of scapholunate dissociation and rotatory subluxation of the scaphoid bone, resulting in radioscaphoid malalignment, progressive chondromalacia, and osteoarthritis (39). Sagittal reformatted images from multidetector CT arthrographic data are particularly useful in demonstrating abnormal angulations of the scaphoid and lunate bones (increased scapholunate angle and dorsal or volar intercalated segment instability deformity), radioscaphoid incongruity, cartilage loss, and subchondral bone degenerative changes (Fig 14). Scaphoid nonunion advanced collapse is similar, except that functional scapholunate dissociation results from scaphoid nonunion (Fig 15).

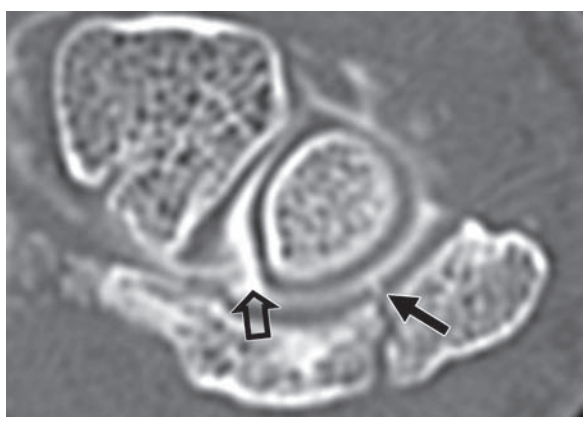

Figure 12. Recent articular fracture of the radial styloid process. Transverse multidetector CT arthrogram shows a fracture line and cartilage disruption (solid arrow) with an associated scapholunate ligament tear (open arrow).

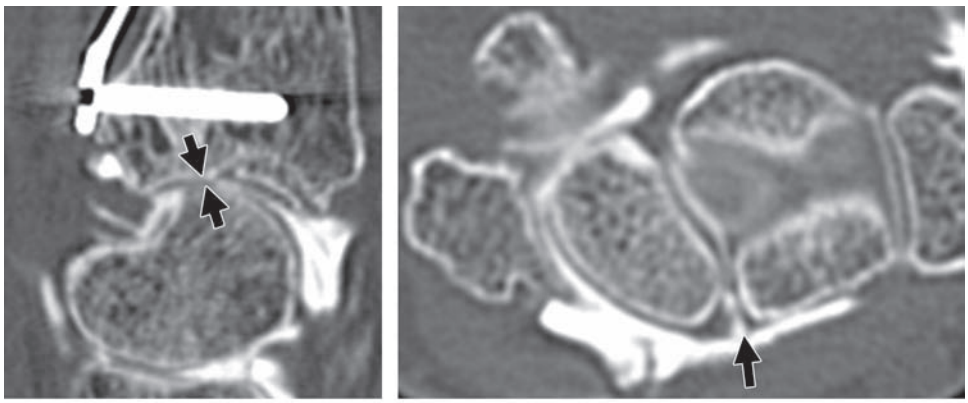

a. b.

Figure 13. Articular derangement in a 54-year-old man who presented with persistent pain after undergoing anterior placement of a bone plate for articular fracture of the radius. Sagittal **(a)** and transverse **(b)** reformatted images from multidetector CT arthrographic data demonstrate cartilage step-off with early osteoarthritis (arrows in **a**) and a scapholunate ligament tear (arrow in **b**). Note the absence of metallic hardware–related artifacts.

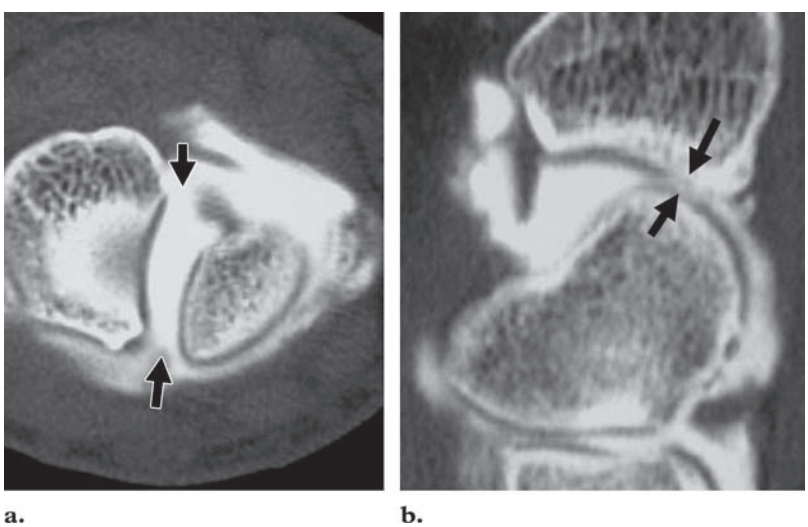

a. b.

Figure 14. Complete scapholunate ligament tear. Transverse **(a)** and sagittal **(b)** multidetector CT arthrograms show a complete scapholunate ligament tear (arrows) with scapholunate dissociation and rotatory subluxation of the scaphoid bone. Early cartilage degeneration reflects evolution toward scapholunate advanced collapse.

Figure 15. Scaphoid nonunion advanced collapse deformity. Coronal multidetector CT arthrogram shows scaphoid nonunion (white arrows) resulting in radioscaphoid osteoarthritis beginning at the radial styloid process (black arrows).

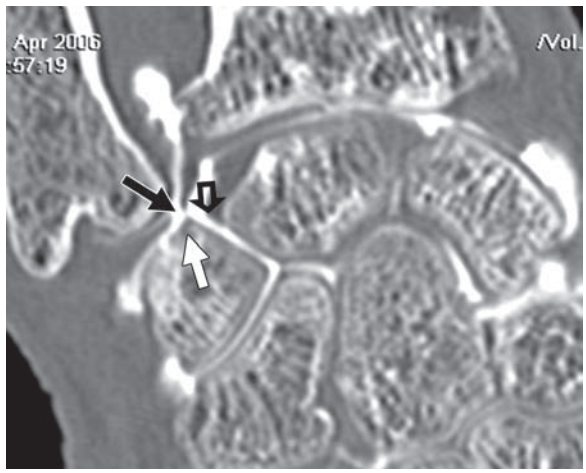

Figure 16. Ulnocarpal impaction syndrome following traumatic shortening of the radius. Multidetector CT arthrogram shows that relative ulnar lengthening has caused central perforation of the triangular fibrocartilage (solid black arrow), a lunotriquetral ligament tear (open black arrow), and triquetral chondromalacia (white arrow).

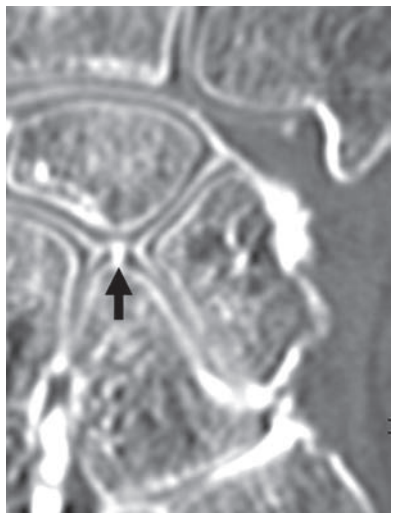

Figure 17. Hamatolunate impingement. Coronal multidetector CT arthrogram shows chondromalacia of the tip of the hamate bone (arrow).

Ulnocarpal Impaction Syndrome

Ulnocarpal abutment is common but not always symptomatic. It results from either a constitutional (positive variance) or relative acquired (radial shortening following fracture) long ulna. Imaging features are described as Palmer class II and include positive ulnar variance, central wear or tear of the triangular fibrocartilage, chondromalacia of the adjacent lunate bone and ulnar head with subchondral bone abnormalities, lunotriquetral ligament tear, and ulnocarpal or DRUJ osteoarthritis (Fig 16) (40).

Hamatolunate Impingement

Hamatolunate impingement occurs only when the lunate bone has an accessory hamate facet (type 2 lunate bone, present in two-thirds of the population). Chondromalacia of the proximal hamate bone is observed in about 50% of cases but is usually asymptomatic (Fig 17) (41,42).

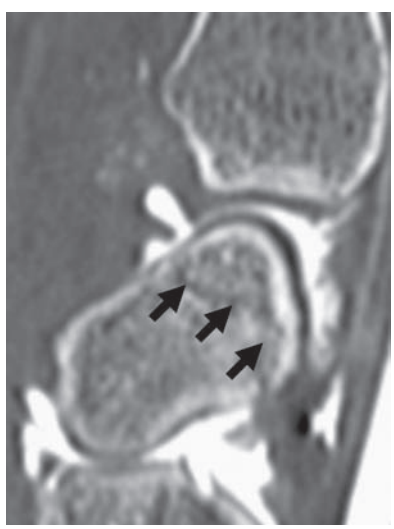

Figure 18. Occult scaphoid fracture. Sagittal multidetector CT arthrogram clearly shows a fracture line (arrows) that was not apparent on earlier radiographs or CT scans.

Bone Abnormalities

Although multidetector CT arthrography is not intended for use in searching for bone fractures, detection of occult fractures is common. Scaphoid fracture is the most common fracture of the carpal bones and can be discovered incidentally when looking for a scapholunate ligament tear (Fig 18). Small avulsion fractures that are usually overlooked with other imaging techniques are well depicted with multidetector CT arthrography. Other bone abnormalities are uncommon. Giant intraosseous ganglion cyst may be present, occasionally causing pathologic fracture (Fig 19). Finally, patients with bone fixation can be imaged with multidetector CT arthrography to evaluate bone healing and hardware, as well as associated cartilage and ligament injuries (Fig 20).

Soft-Tissue Abnormalities

Detection of soft-tissue abnormalities is obviously the Achilles' heel of multidetector CT arthrography

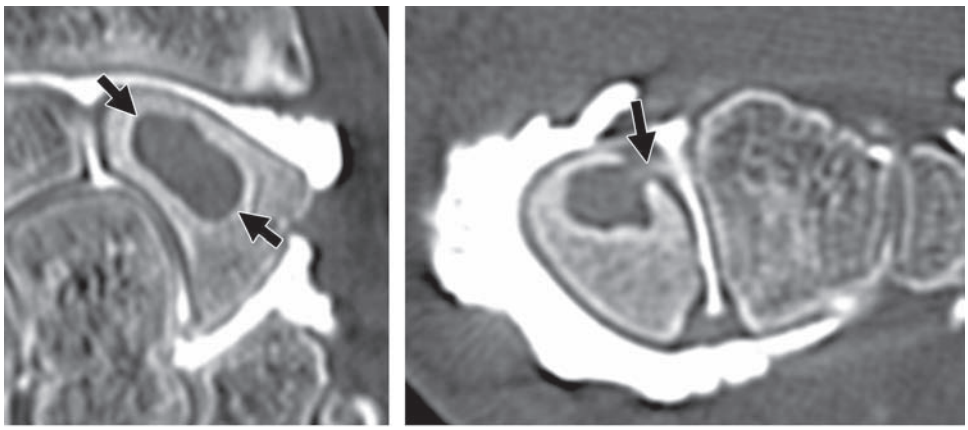

a. b.

Figure 19. Intraosseous ganglion cyst. Coronal **(a)** and sagittal **(b)** multidetector CT arthrograms show a large ganglion cyst of the scaphoid bone (arrows in **a**) communicating with the scapholunate space (arrow in **b**). Such large cysts create a risk for pathologic fracture.

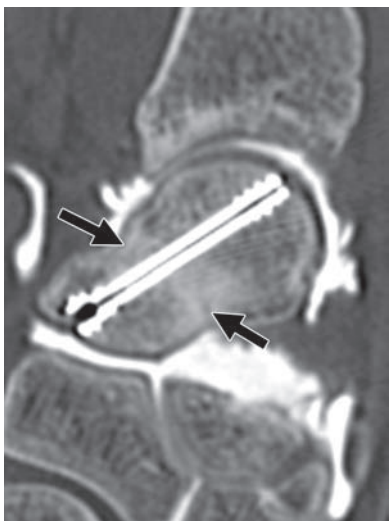

Figure 20. Evaluation of a patient with bone fixation. Sagittal oblique baseline multidetector CT arthrogram obtained after scaphoid fixation with a Herbert screw clearly depicts the screw as well as the healed fracture line (arrows).

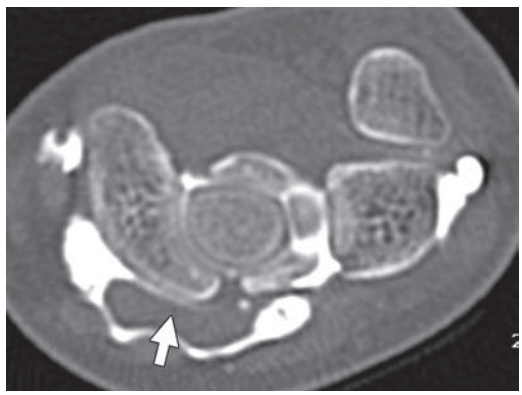

Figure 21. Inconsistent enhancement of a ganglion cyst. Transverse multidetector CT arthrogram shows a large, unenhanced ganglion cyst (arrow) that has developed from the dorsal portion of the scapholunate ligament.

and may require additional MR imaging or ultrasonographic investigation. Ganglion cysts are inconsistently enhanced with contrast media (Fig 21). Multidetector CT arthrography is also largely insensitive to tendon abnormalities.

Conclusions

Multidetector CT arthrography of the wrist joint is helpful in the investigation of a wide range of articular disorders. A basic knowledge of the relevant anatomy, pathophysiologic features, and imaging technique is mandatory for obtaining high-yield diagnostic information.

References

1. Moser T, Dosch J, Moussaoui A, Dietemann J. Wrist ligament tears: evaluation of MRI and combined MDCT and MR arthrography. AJR Am J Roentgenol 2007;188:1278–1286.
2. Schmid MR, Schertler T, Pfirrmann CW, et al. Interosseous ligament tears of the wrist: comparison of multi–detector row CT arthrography and MR imaging. Radiology 2005;237:1008–1013.
3. Brown RR, Fliszar E, Cotten A, Trudell D, Resnick D. Extrinsic and intrinsic ligaments of the wrist: normal and pathologic anatomy at MR arthrography with three-compartment enhancement. RadioGraphics 1998;18:667–674.
4. Rominger MB, Bernreuter WK, Kenney PJ, Lee DH. MR imaging of anatomy and tears of wrist ligaments. RadioGraphics 1993;13:1233–1246.
5. Kauer JM. Functional anatomy of the wrist. Clin Orthop Relat Res 1980;149:9–20.

6. Berger RA. The gross and histologic anatomy of the scapholunate interosseous ligament. J Hand Surg [Am] 1996;21:170–178.
7. Palmer AK, Werner FW. The triangular fibrocartilage complex of the wrist: anatomy and function. J Hand Surg [Am] 1981;6:153–162.
8. Palmer AK, Glisson RR, Werner FW. Relationship between ulnar variance and triangular fibrocartilage complex thickness. J Hand Surg [Am] 1984; 9:681–682.
9. Berger RA, Landsmeer JM. The palmar radiocarpal ligaments: a study of adult and fetal human wrist joints. J Hand Surg [Am] 1990;15:847–854.
10. Viegas SF. The dorsal ligaments of the wrist. Hand Clin 2001;17:65–75.
11. Mayfield JK. Patterns of injury to carpal ligaments: a spectrum. Clin Orthop Relat Res 1984;187:36–42.
12. Theumann NH, Etechami G, Duvoisin B, et al. Association between extrinsic and intrinsic carpal ligament injuries at MR arthrography and carpal instability at radiography: initial observations. Radiology 2006;238:950–957.
13. Zlatkin MB, Rosner J. MR imaging of ligaments and triangular fibrocartilage complex of the wrist. Magn Reson Imaging Clin N Am 2004;12:301–331.
14. Ruch DS, Poehling GG. Arthroscopic management of partial scapholunate and lunotriquetral injuries of the wrist. J Hand Surg [Am] 1996;21:412–417.
15. Watson HK, Weinzweig J, Zeppieri J. The natural progression of scaphoid instability. Hand Clin 1997;13:39–49.
16. Meade TD, Schneider LH, Cherry K. Radiographic analysis of selective ligament sectioning at the carpal scaphoid: a cadaver study. J Hand Surg [Am] 1990;15:855–862.
17. Ritt MJ, Linscheid RL, Cooney WP 3rd, Berger RA, An KN. The lunotriquetral joint: kinematic effects of sequential ligament sectioning, ligament repair, and arthrodesis. J Hand Surg [Am] 1998; 23:432–445.
18. Ritt MJ, Bishop AT, Berger RA, Linscheid RL, Berglund LJ, An KN. Lunotriquetral ligament properties: a comparison of three anatomic subregions. J Hand Surg [Am] 1998;23:425–431.
19. Ruegger C, Schmid M, Pfirrmann C, Nagy L, Gilula L, Zanetti M. Peripheral tear of the triangular fibrocartilage: depiction with MR arthrography of the distal radioulnar joint. AJR Am J Roentgenol 2007;188:187–192.
20. Zanetti M, Linkous MD, Gilula LA, Hodler J. Characteristics of triangular fibrocartilage defects in symptomatic and contralateral asymptomatic wrists. Radiology 2000;216:840–845.
21. Lee DH, Dickson KF, Bradley EL. The incidence of wrist interosseous ligament and triangular fibrocartilage articular disc disruptions: a cadaveric study. J Hand Surg [Am] 2004;29:676–684.
22. Mikic ZD. Age changes in the triangular fibrocartilage of the wrist joint. J Anat 1978;126:367–384.
23. Linkous MD, Pierce SD, Gilula LA. Scapholunate ligamentous communicating defects in symptomatic and asymptomatic wrists: characteristics. Radiology 2000;216:846–850.
24. Wilson AJ, Gilula LA, Mann FA. Unidirectional joint communications in wrist arthrography: an evaluation of 250 cases. AJR Am J Roentgenol 1991; 157:105–109.
25. Gilula LA, Hardy DC, Totty WG. Distal radioulnar joint arthrography. AJR Am J Roentgenol 1988; 150:864–866.
26. Tirman RM, Weber ER, Snyder LL, Koonce TW. Midcarpal wrist arthrography for detection of tears of the scapholunate and lunotriquetral ligaments. AJR Am J Roentgenol 1985;144:107–108.
27. Levinsohn EM, Rosen ID, Palmer AK. Wrist arthrography: value of the three-compartment injection method. Radiology 1991;179:231–239.
28. Yin YM, Evanoff B, Gilula LA, Pilgram TK. Evaluation of selective wrist arthrography of contralateral asymptomatic wrists for symmetric ligamentous defects. AJR Am J Roentgenol 1996;166:1067–1073.
29. Totterman SM, Miller RJ. Scapholunate ligament: normal MR appearance on three-dimensional gradient-recalled-echo images. Radiology 1996;200: 237–241.
30. Smith DK. Scapholunate interosseous ligament of the wrist: MR appearances in asymptomatic volunteers and arthrographically normal wrists. Radiology 1994;192:217–221.
31. Smith DK, Snearly WN. Lunotriquetral interosseous ligament of the wrist: MR appearances in asymptomatic volunteers and arthrographically normal wrists. Radiology 1994;191:199–202.
32. Totterman SM, Miller RJ. Triangular fibrocartilage complex: normal appearance on coronal three-dimensional gradient-recalled-echo MR images. Radiology 1995;195:521–527.
33. Limb D, Agrawal Y. The distribution of bone islands and juxta-articular bone cysts in the growing hand. J Hand Surg [Br] 2006;31:441–444.
34. Resnik CS, Grizzard JD, Simmons BP, Yaghmai I. Incomplete carpal coalition. AJR Am J Roentgenol 1986;147:301–304.
35. Timins M, Jahnke J, Krah S, Erickson S, Carrera G. MR imaging of the major carpal stabilizing ligaments: normal anatomy and clinical examples. RadioGraphics 1995;15:575–587.
36. Schmitt R, Froehner S, Coblenz G, Christopoulos G. Carpal instability. Eur Radiol 2006;16:2161–2178.
37. Palmer AK. Triangular fibrocartilage complex lesions: a classification. J Hand Surg [Am] 1989;14: 594–606.
38. Goldfarb CA, Yin Y, Gilula LA, Fisher AJ, Boyer MI. Wrist fractures: what the clinician wants to know. Radiology 2001;219:11–28.
39. Watson HK, Ballet FL. The SLAC wrist: scapholunate advanced collapse pattern of degenerative arthritis. J Hand Surg [Am] 1984;9:358–365.
40. Cerezal L, del Pinal F, Abascal F, Garcia-Valtuille R, Pereda T, Canga A. Imaging findings in ulnar-sided wrist impaction syndromes. RadioGraphics 2002;22:105–121.
41. Malik AM, Schweitzer ME, Culp RW, Osterman LA, Manton G. MR imaging of the type II lunate bone: frequency, extent, and associated findings. AJR Am J Roentgenol 1999;173:335–338.
42. Viegas SF, Patterson RM, Hokanson JA, Davis J. Wrist anatomy: incidence, distribution, and correlation of anatomic variations, tears, and arthrosis. J Hand Surg [Am] 1993;18:463–475.

This article meets the criteria for 1.0 credit hour in category 1 of the AMA Physician's Recognition Award. To obtain credit, see accompanying test at http://www.rsna.org/education/rg_cme.html.

Multidetector CT Arthrography of the Wrist Joint: How to Do It

Thomas Moser, MD, et al

RadioGraphics 2008; 28:787–800 • **Published online** 10.1148/rg.283075087 • **Content Codes:** CT MK

Page 788

The wrist joint is considered to be the most complex articulation in the human body. However, its anatomy can be simplified into three major compartments: the distal radioulnar joint (DRUJ), the radiocarpal joint, and the midcarpal joint. The radiocarpal joint involves the distal radius and the proximal carpal row; the midcarpal joint involves the proximal and distal carpal rows. Their combined motion is synergistic and comparable to that of a spheroidal joint, allowing flexion (volar flexion), extension (dorsal flexion), and radial and ulnar deviations of the wrist. Along with its proximal counterpart, the DRUJ is responsible for pronation and supination of the forearm.

Page 789

Precise delineation of the extent of a tear is feasible with modern imaging techniques, and most authors now differentiate between complete (all three portions disrupted) and incomplete (one or two portions disrupted, also referred to as "partial" by some authors) interosseous ligament tears (1,12,13). This distinction is clinically relevant, since most patients who present with incomplete tears have no wrist instability and can be treated conservatively (14,15). Experimental studies have demonstrated that disruption of both interosseous and capsular ligaments is needed to cause wrist instability (16,17). However, not all incomplete tears are equally negligible. The dorsal portion of the scapholunate ligament and the volar portion of the lunotriquetral ligament are essential for wrist stability, whereas the membranous proximal portions have virtually no mechanical importance (6,18). Further classification of ligament tears helps differentiate full-thickness (usually communicating) tears from partial-thickness (noncommunicating) tears (Fig 2). The pathologic significance of partial-thickness tears for interosseous ligaments is discussed in the literature, but the significance of such tears is widely considered to be greater for the TFCC (19,20).

Page 790

Multidetector CT arthrography currently allows the direct visualization of ligament tears. Even partial-thickness tears can be recognized when both adjacent compartments are enhanced. The classic abnormal communication has actually lost its semeiologic importance, since ligament tears are directly visualized. Our examination protocol typically includes initial enhancement of the midcarpal compartment and, if a TFCC tear is suspected, enhancement of the DRUJ. The radiocarpal compartment is punctured only if spontaneous enhancement through a tear does not occur (1,28).

Page 793

A tear varies in appearance depending on its extent. Full-thickness tears are usually communicating (unless the defect is plugged by a scar) and manifest as an interruption of the ligament underlined by iodinated contrast material. The stump of the ligament can be seen floating freely in cases of recent tear but then progressively disappears over time. Assessment of the stump can be useful for guiding reconstructive surgery. Partial-thickness tears are noncommunicating and therefore require enhancement of both adjacent compartments for adequate depiction. They manifest as abnormal thinning, superficial fraying, or irregularities on one side of the ligament (Fig 8a, 8b). Ganglion cyst formation from a partial-thickness tear is also frequently observed in the dorsal portion of the scapholunate ligament. These cysts can be very small and unenhanced, being identified only on the basis of focal bulging of the dorsal scapholunate ligament in its lower aspect (Fig 8c, 8d).

Page 796

Cartilage abnormalities are exquisitely depicted with multidetector CT arthrography. Acute traumatic lesions are usually associated with articular fractures (Fig 12). Persistent incongruity is a major source of articular derangement, and the maximum tolerable step-off is less than 2 mm (Fig 13). Early cartilage degeneration also occurs as a result of loss of radial inclination and volar tilt or radial shortening with relative lengthening of the ulna (38). Degenerative lesions are the result of excessive strain over articular surfaces caused by posttraumatic instability or malalignment. Various patterns can be recognized, including radioscaphoid osteoarthritis, ulnocarpal impaction syndrome, and hamatolunate impingement.